Numerical evaluation of multi-layered solid-PCM thermocline-like tanks as thermal energy storage systems for CSP applications

P. Galione[a, b], C. Pérez-Segarra[a], I. Rodríguez[a], S. Torras[a], J. Rigola[a]

[a]*Heat and Mass Transfer Technological Center (CTTC) Universitat Politècnica de Catalunya – BarcelonaTech, ETSEIAT, Colom 11, Terrassa (Barcelona) 08222, Spain*
[b]*Instituto de Ingeniería Mecánica y Producción Industrial (IIMPI), Facultad de Ingeniería, Universidad de la República (UdelaR), Julio Herrera y Reissig 565, Montevideo 11300, Uruguay*

Abstract

The two-tank system is the technology used for thermal energy storage (TES) in current concentrating solar power (CSP) plants. Thermocline storage concept has been considered for more than a decade as a possible solution to reduce the high cost of the storage system in these plants. In previous works, multi-layered solid-PCM (MLSPCM) thermocline-like storage tank configurations has been introduced and studied, giving promising results for their use as thermal energy storage systems for CSP. In this work, further analysis is performed in the use of this new concept of TES, by considering variable inlet conditions, and simulating the tank shell and the foundation. The numerical simulations are based on a modular object-oriented methodology. Energetic and exergetic results are presented and compared against a reference 2-tank case and against different thermocline configurations with either solid or phase change filler materials. Again, promising results are obtained for the tested MLSPCM concept.

1. Introduction

Thermal energy storage systems are an essential feature to make an efficient use of solar energy due to the inherent intermittence of this energy source. For concentrated solar power plants the current standard thermal storage system is the two-tank molten salt. Thermocline storage system has also been considered as an alternative that would

result in lower costs, since it consists of a single tank instead of two and a high amount of the expensive molten salt could be replaced by a cheaper solid filler material. Encapsulated phase change materials (PCM) can also be used to store energy, using less storage material than would be used with a sensible energy storage medium.

Nomenclature

A	Surface area	x	Axial direction
C_p	Specific heat capacity		
D	Diameter	*Greek letters*	
ex	Exergy	ε	Porosity
f	Liquid fraction	ρ	Density
F	Filled fraction of PCM capsules	η	Efficiency
h	Enthalpy		
H	Height	*Subscripts*	
k	Thermal conductivity	ext	Ambient conditions
L	Latent heat of fusion	f	Heat transfer fluid
$\dot{m}$	Mass flow rate	$fill$	Filler material
n_{cap}	Number of capsules	i	Index of tank section
r	Radial direction	in	Inlet conditions
R_{conv}, R_{cond}	Convection and conduction thermal resistances between the HTF and the capsules/particles	l	Liquid phase
		out	Outlet conditions
		PB	Power block
t	Time	s	Solid phase
T	Temperature	SF	Solar field
U_{TC-Tsh}	Global heat transfer coefficient between the HTF and the tank shell	tk	Tank
		TSh	Tank shell
V	Volume		

In previous works [1, 2], a novel multi-layered solid-PCM (MLSPCM) thermocline-like storage tank concept was introduced (Fig. 1). Thermal performance was evaluated by means of numerical simulations, allowing to conclude that this new concept is a promising alternative to 2-tank and standard thermocline TES.

In this work, further analysis is carried out by evaluating the thermal performance of selected MLSPCM prototypes over several days, for which variable inlet conditions are defined, mimicking the behavior of a typical CSP plant. Thermal losses to the ambient through the tank shell and foundation are considered, as well as the thermocline degradation in the "idle" periods (when no fluid flow is entering or leaving the tank, e.g. during the night, after a complete discharge of the tank has been carried out).

2. Mathematical model

The thermocline-like TES considered are formed by different elements, e.g thermocline packed bed (filler material and HTF), tank foundation and tank walls, which interact with each other through their boundary conditions. This implementation has been performed within the NEST platform [3], which allows the linking between different elements of the thermal system. The mathematical model considers the transient behaviour of the thermocline-like packed beds, the tank walls and insulation, taking into account the variable outdoor conditions (DNI, ambient temperature). A brief mathematical description is presented hereafter.

2.1. TES tanks

Mass, momentum and energy conservation equations have to be solved in order to be able to simulate the thermal behavior of a thermocline-like tank. Some simplifying assumptions are made and empirical correlations are used. Most relevant assumptions are:

- One-dimensional fluid flow and temperature distribution (in the flow direction).
- One-dimensional heat transfer in filler particles/capsules (radial direction).
- Spherical shape of filler particles/capsules.
- Constant density of both fluid and filler bed materials (solid and PCM).
- Heat conduction between different filler material particles/capsules is not considered.
- Negligible radiation transfer.

The one-dimensionality in the fluid results in an axially-varying fluid temperature map. In the filler particles/capsules, a radial variation of the temperature is assumed, which also depends on the axial position in the tank.

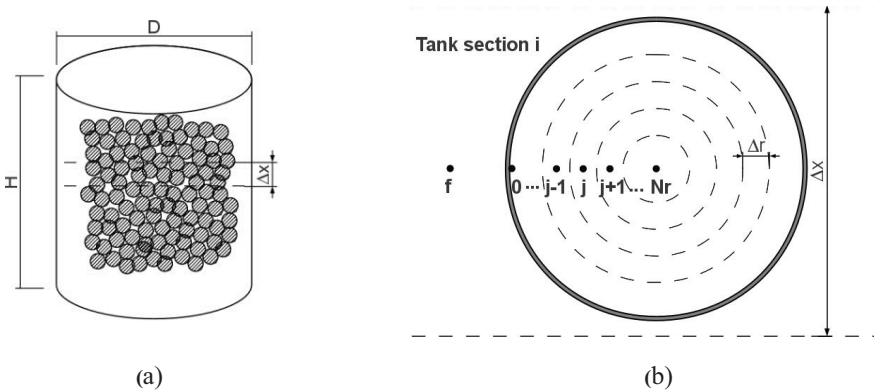(a)   (b)

Fig. 1. (a) Sketch representing the cylindrical container with the PCM capsules packed in a random fashion; (b) discretization details of the tank and of a representative particle/capsule, indicating the sub-indices used for tank sections (*i*) and capsule control volumes (*j*).

For determining the temperature of the heat transfer fluid (HTF) and of the filler material, the energy conservation equations are discretized using the Finite Volume Method. The tank is divided in transversal cylindrical sections of equal height (Δx), as sketched in Fig. 1(a). In each tank section, a single particle/capsule needs to be simulated, as all are affected by the same fluid temperature, due to one-dimensionality assumption. This filler particle, assumed as spherical, is discretized in the radial direction in *Nr* control volumes, as shown in Fig. 1(b).

2.1.1. Equations of the TES tanks:

The energy balance of the HTF in the ith tank section result in:

$$\rho_f \varepsilon_i V_i C_{p,f} \frac{\partial T_{i,f}}{\partial t} = \left(A k_{eff} \frac{\partial T}{\partial x}\right)\Big|_{i-1/2}^{i+1/2} - \dot{m} C_{p,f} (T_{i+1/2,f} - T_{i-1/2,f}) - n_{cap,i} \frac{(T_{i,f} - T_{i,0})}{R_{conv,i} + R_{cond,i}} \\ - U_{TC-TSh}(T_{i,f} - T_{i,TSh}) \tag{1}$$

where $T_{i,0}$ is the temperature of the internal surface of the particles/capsules (boundary node in Fig. 1b). In the advective term (second in the right hand side) the fluid is assumed to be coming from section *i−1* and going to section *i+1*. The diffusive term (first in the right hand side) uses the effective thermal conductivity (k_{eff}), which takes into account the thermal dispersion and the effect of the conductivity of the filler material, as indicated in [4]. R_{conv} is the convective thermal resistance between the HTF and the particles/capsules, which is calculated as in [4]; while R_{cond} is the conductive thermal resistance of the capsules shells, which is zero for the solid filler particles.

The energy balances for the inner nodes ($j = 1...N_r$) of the filler materials (either PCM capsules or solid particles) remain:

$$\rho_{fill} V_{i,j} F_i \frac{\partial h_{i,j}}{\partial t} = \left(k_{fill} A \frac{\partial T}{\partial r} \right)\bigg|_{i,j-1/2} - \left(k_{fill} A \frac{\partial T}{\partial r} \right)\bigg|_{i,j+1/2} \tag{2}$$

while for the boundary node ($j = 0$), in contact with the heat transfer fluid, results in:

$$\rho_{fill} V_{i,0} F_i \frac{\partial h_{i,0}}{\partial t} = \frac{T_{i,f} - T_{i,0}}{R_{conv,i} + R_{cond,i}} - \left(k_{fill} A \frac{\partial T}{\partial r} \right)\bigg|_{i,1/2} \tag{3}$$

where the F indicates the filled fraction of the PCM capsules, which is between 0 and 1 and accounts for the void space needed to allow for the thermal expansion in the melting.

In order to solve these equations it is necessary to define a relation between the enthalpy and the temperature of the filler materials (solid and/or PCM). Considering constant specific heats for each phase, these relations are:

$$h - h_0 = C_{p,s}(T - T_0) \qquad\qquad T < T_s \tag{4}$$

$$h - h_0 = C_{p,s}(T - T_0) + fL \qquad\qquad T_s < T < T_{sl} \tag{5}$$

$$h - h_0 = C_{p,l}(T - T_{sl}) + C_{p,s}(T_{sl} - T_0) + fL \qquad\qquad T_{sl} < T < T_l \tag{6}$$

$$h - h_0 = C_{p,l}(T - T_{sl}) + C_{p,s}(T_{sl} - T_0) + L \qquad\qquad T_l < T \tag{7}$$

$$f = \frac{T - T_s}{T_l - T_s} \tag{8}$$

T_{sl} indicates the temperature in the phase change range beyond which the material has a mostly liquid behavior, and below which it behaves mostly as solid. f is the liquid fraction, whose values go from 0 (pure solid) to 1 (pure liquid) and L is the latent heat of fusion. Since T_s and T_l are not the same, these equations are meant to model PCMs with a fusion temperature range. However, taking a very narrow temperature range, fixed fusion temperature PCMs can also be modeled with this approach. Hence, a unique value of h exists for each value of T, and the energy balance equations may be expressed with T as the only variable.

It should be noted that with this strategy an explicit tracking of the liquid-solid interface is avoided, since its location is implicitly determined by values of f between 0 and 1 (indicating a solid-liquid mixture).

The exergy global balance of the heat transfer fluid is calculated in the following manner:

$$\dot{m}(ex_{out} - ex_{in}) = \dot{m} C_{p,f} \left(T_{out} - T_{in} - T_{ref} ln \frac{T_{out}}{T_{in}} \right) \tag{9}$$

where sub-indices *out* and *in* correspond to the properties of the fluid exiting or entering the tank, respectively. *ex* is the exergy, and T_{ref} the reference temperature considered as the "ambient" for the determination of the exergy.

The resulting exergy flow is the difference between the exergy exiting and entering the tank with the fluid, which can be used in the power block for producing electricity.

2.2. Tank walls, insulation and foundation

A transient heat balance is performed to find the temperature of the tank walls (container + insulation) in each tank section. For the foundation, a simplified zonal model has been used. More details about the formulation for these components can be found in [5] and [6].

3. Cases definition

Tanks are designed to operate in a CSP plant similar to Andasol 1 in Granada, Spain. The parameters for this reference plant are shown in Table 1. The heat transfer fluid passing through the TES is molten salt. A sketch of the plant working with a TES of a single tank is shown in Fig. 2. Operating conditions of the TES that are considered here are shown in Table 2, while the thermo-physical properties of the different materials in the packed beds (filler materials and heat transfer fluid) are indicated in Table 3. The efficiency of the heat exchanger is assumed to be 1.
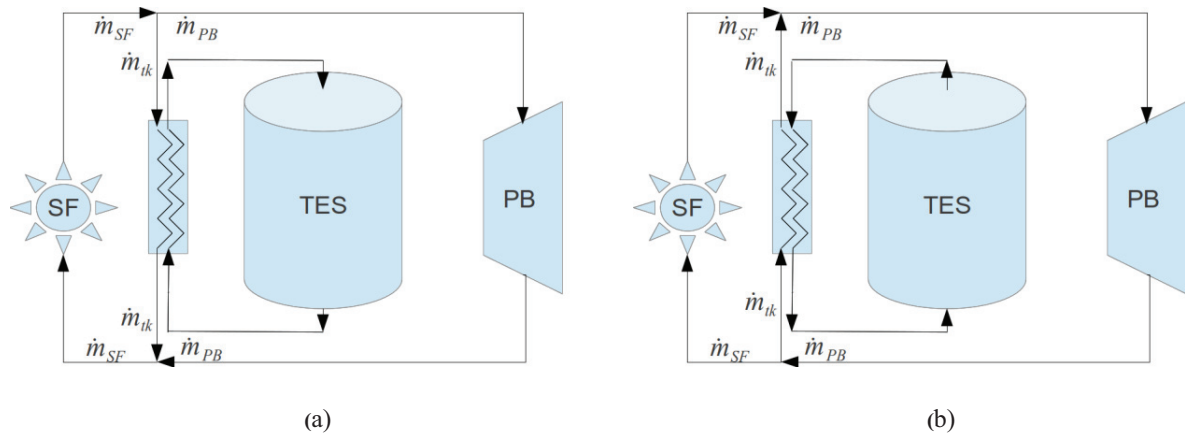

Fig. 2. Simplified sketches of CSP plant with single-tank TES. (a) charge process; (b) discharge process.

Table 1. Parameters of CSP plant

Characteristics	Reference CSP plant
Turbine nominal power (MW_{el})	50
Technology	Parabolic trough
Solar field area, A_{SF} (m^2)	510,120
Solar Field efficiency (peak)	70%
Power Block efficiency (peak)	38%
Storage capacity with 2-tank system (13x38 m) (MWh)	1152

Operating temperatures and threshold values for the temperature of the fluid going to the power block (PB) and to the solar field (SF) are defined in Table 2. If the temperature goes below (discharge) or above (charge) these values, then the corresponding process is ended. A difference between this criterion and that of previous works [1, 2] is that these threshold temperatures are not compared directly the temperatures of the fluid coming out of the TES tank, but to that of the mixture of the fluids from the tank and from the PB (charge) or SF (discharge).

These thresholds define two admissible temperature intervals, one for the temperature of the fluid going to the SF (charge) and another for that going to the PB (discharge). Here, both admissible ranges have been assumed to be 15% of the maximum temperature interval (100ºC); e.g. 290-305ºC for the SF and 375-390ºC for the PB.

Furthermore, to avoid several charge and discharge processes being started and stopped in small time intervals, different (more restrictive) thresholds have been defined for starting the processes; i.e. a discharge is not started if the temperature at the top of the tank is lower than 380ºC, while the charge is not started if the temperature at the bottom of the tank is higher than 300ºC.

The initial conditions for the TES, in the first day of simulation, are uniform temperatures of 290ºC for the tank and 15 ºC for the soil.

Table 2. Operating conditions

Temperature of hot molten salt (ºC)	390
Temperature of cold molten salt (ºC)	290
Threshold temperature for ending discharge (to Power Block) (ºC)	375
Threshold temperature for ending charge (to Solar Field) (ºC)	305
Threshold temperature for starting discharge (to Power Block) (ºC)	380
Threshold temperature for starting charge (to Solar Field) (ºC)	300

Table 3. Thermo-physical properties of the different materials

	ρ (kg/m3)	C_{ps} (J/kg K)	C_{pl} (J/kg K)	k_s (W/m K)	k_l (W/m K)	L (J/kg)
Quarzite rock & sand (Qu)	2500	830	-	5.69	-	-
PCM (KOHXXX)	2040	1340	1340	0.5	0.5	1.34×10^5
Molten salt	1873.8	-	1501.5	-	$0.443 + 1.9 \times 10^{-4} \times T(ºC)$	-

3.1. Operation control

The simulations are carried out for 17 days in summer (from 30, June to 17 July) in Seville, Spain. The direct normal irradiance (DNI) and rest of weather data is obtained from the software METEONORM [7]. Table 4 depicts some basic information for this location. For determining the mass flow coming from the solar field, the following equation is used:

$$\dot{m}_{SF} = \frac{DNI.A_{SF}.\eta_{SF}}{C_p \Delta T_{SF}} \tag{10}$$

where the DNI is multiplied by an overall efficiency for the solar field (η_{SF}), which in this case is taken as 0.7. This is the peak value for the efficiency of the solar field in Andasol 1 plant [8]. The hot fluid coming out of the SF is set at a fixed temperature of 390ºC, while the cold fluid entering the SF, which is a mixture of that coming from the PB and that going out of the tank (in the charging processes), has a variable temperature.

It is assumed that the mass flow coming from the SF is directly sent to generate vapor in the power block until it is higher than that needed to generate the nominal power in the PB. From this point on, the excess flow is sent to charge the TES. When the mass flow from the SF is not enough to reach the nominal power in the PB, the discharge of the TES is started, and the mass flow passing through the TES is the difference between that coming from the SF and that needed for generating nominal power in the PB.

The discharge of the TES is continued until the threshold temperature is reached. After this, an idle (or standby) process starts, in which no flow passes through the tank, until there is excess energy to charge again the TES.

Table 4. Location with basic data.

Location	Latitude (º)	Longitude (º)	July		
			T_{max} (ºC)	T_{min} (ºC)	DNI (kWh/m²day)
Seville, Spain	37.37	5.97	39.6	16.2	7.58

3.2. TES configurations

Table 5 shows the different cases (prototypes) considered and simulated. Each is assigned with a code. 2-TANK refers to the standard 2-tank molten salt system, with dimensions of 13m height and 38 m diameter. A1 is a solid-filled thermocline tank with the same dimensions. B1 to B3 are tanks filled with a single encapsulated PCM. C1 is a MLSPCM configuration with 3 layers (see sketch in Fig. 2) and the same dimensions, while C2 is a MLSPCM with the same layer configuration but with a higher diameter. Finally, case A2 is the solid-filled thermocline with the same dimensions as C2.

The material for the tanks is assumed to be steel A516gr70, while Spintex342G-100 is used as insulation material for the lateral and roof walls. The insulation material is covered with a thin layer of aluminium 2024 T6.

Details about geometry used in all the cases are given hereafter:
- Vertical wall thickness, e = 0.039 m.
- Bottom wall thickness, e = 0.021 m.
- Insulation thickness: e = 0.4 m.
- Foundation thicknesses: dry sand, e = 0.006 m; foam-glass, e = 0.420 m; heavy weight concrete, e = 0.450 m; soil, e = 9.140 m.

The PCM of the top layers in the MLSPCM prototypes is indicated as KOH380, which corresponds to a fictitious PCM with the same properties as those of the KOH, except for its fusion temperature which is set to 380ºC. For the bottom layer, KOH300 is chosen, i.e. a fictitious KOH with a fusion temperature of 300ºC.

The porosities considered for the solid-filled layers is 0.22, while for the layers with PCM capsules is 0.4, and the representative particle/capsules diameters are 0.015 m.

Table 6 indicates the mass of filler material and HTF confined inside each tank, while Table 7 shows the theoretical storage capacity of each configuration, considering the amount of sensible and latent heat storable in the temperature range of 290-390ºC.

Table 5. Codification used for the different cases. Materials KOH300 and KOH380 are fictitious PCM whose fusion temperatures are indicated by the number (300ºC and 380ºC) and rest of properties are equal to those of KOH (whose fusion temperature is 360ºC). Qu is for a mixture of quartzite rock & sand, as in Pacheco et al., 2002.

TES concept – Filler materials (proportionª) – Dimensions	Code
2-tank Molten Salt – no filler – 13x38m, adiabatic conditions	2-TANK
Thermocline – Qu (100%) – 13x38m	A1
PCM – KOH (100%) – 13x38m, volume of capsules filled = 100%	B1
PCM – KOH380 (100%) – 13x38m, volume of capsules filled = 85%	B2
PCM – KOH300 (100%) – 13x38m, volume of capsules filled = 85%	B3
MLSPCM – KOH380-Qu-KOH300 (5%-90%-5%) – 13x38m, volume of capsules filled = 85%	C1
MLSPCM – KOH380-Qu-KOH300 (5%-90%-5%) – 13x43.7m, volume of capsules filled = 85%	C2
Thermocline – Qu (100%) – 13x43.7m	A2

Table 6. Mass confined inside the tank for the different test cases

MASS DATA	2-TANK	A1	B1	B2	B3	C1	C2	A2
Mass of PCM (ton)	0	0	15310	13013	13013	5255	1721	0
Mass of Quartzite & sand (ton)	0	28750	0	0	0	17139	34219	38022
Mass of confined HTF (ton)	27629	6078	11052	11052	11052	8087	8696	8039

ª The proportion of each material indicated between brackets (in the same order as the filler materials) is the proportion of total height occupied by the corresponding filler material.

Table 7. Maximum storable energy for the different test cases

STORAGE CAPACITY (MWh)	2-TANK	A1	B1	B2	B3	C1	C2	A2
Filler material	0	663	1140	969	969	786	917	877
Confined HTF	1152	254	461	461	461	337	363	335
Total (filler + HTF)	1152	916	1601	1430	1430	1124	1280	1212

4. Numerical results

Table 8[b] shows the results for all the presented cases. These results are mean values, per day, of the 17 days of simulation.

Firstly, it can be seen that the reference 2-tank TES shows zero energy losses, due to being considered as the ideal case, without simulating its thermal losses, i.e. the hot tank is always at 390ºC and the cold tank at 290ºC.

Table 8. Performance results. Mean values per day, for 17 days in summer.

RESULTS	2-TANK	A1	B1	B2	B3	C1	C2	A2
Total energy from SF (MWh)	2798.6	2776.3	2774.5	2775.0	2781.0	2776.6	2776.2	2776.0
Excess energy available for charging TES (MWh)	1151.0	1125.9	1127.7	1127.4	1128.3	1125.9	1126.2	1126.5
Unused available energy (MWh)	191.6	434.7	670.6	335.2	339.5	348.9	168.0	261.1
Delivered Energy to the PB (by the TES) in the Discharge (MWh)	959.4	682.1	415.7	788.3	754.9	770.6	950.2	853.4
Delivered Energy by TES / Storage capacity (%)	83.3	74.4	26.0	55.1	52.8	68.6	74.2	70.4
Energy losses (MWh)	0.0	3.4	3.6	3.3	3.4	3.4	4.2	4.3
Energy losses / Energy Delivered to PB (%)	0,0	0,5	0,9	0,4	0,5	0,4	0.5	0.5
Exergy delivered to PB by the TES (MWh)	460.6	327.1	199.3	376.1	362.0	369.0	455.1	409.3
Exergy delivered / Exergy delivered in 2-tank system (%)	100	71	43	82	79	80	99	89

For the solid-filled thermocline case (A1), with the same dimensions as one tank of the 2-tank system, it can be seen as the values of energy and exergy delivered to the PB are lower (71%). However, the difference is not as high as that found in previous works [1, 2], due to the less restrictive operating conditions for the TES that have been mentioned above, allowing higher temperatures at the outlet in the charge and lower in the discharge (less frequent), due to the mixing of the outlet fluid with that coming from the PB or from the SF, respectively.

For case B1, with a single encapsulated PCM as the filler material whose melting point lies outside from both admissible temperature ranges, the results are much worse, being in agreement with those obtained in [1] and [2]. No void space inside the PCM capsules has been considered in this case.

Cases B2 and B3, also with a single encapsulated PCM, but whose melting points lie inside one of the admissible temperature ranges, the results are much better. This is also in agreement with previous results. However, when compared against the MLSPCM case C1, they are also very similar, or even better than the latter. This is not in agreement with previous results and is also a consequence of the less restrictive operating conditions for the TES.

Nevertheless, the MLSPCM configuration is considered to be preferable to either of the single PCM configurations, due to requiring much less encapsulated PCM, and therefore most probably being significantly less costly.

————

[b] The difference in the values of total energy coming from the SF and available energy for charging between the different cases is due to different interpolation errors associated to different time steps. These errors are always less than 2.5%.

Case C2, which has the same configuration as C1 but with a higher diameter, is seen to result in almost the same amount of exergy delivered to the power block as in the 2-tank case, and therefore it is considered as equivalent to the latter, since it would result in almost the same amount of power generation. The total volume of the C2 tank is only 32% higher than the volume of one tank of the 2-tank system, while the mass of molten salt needed is less than 32% from that of the latter. The efficiency in the use of the thermal capacity (energy delivered/storable) is one of the best among the tested cases (74.2%).

Finally, case A2, having the same dimensions as C2, delivers 89% of the exergy delivered by the ideal 2-tank configuration. This is 10% lower than that achieved by the C2 configuration.
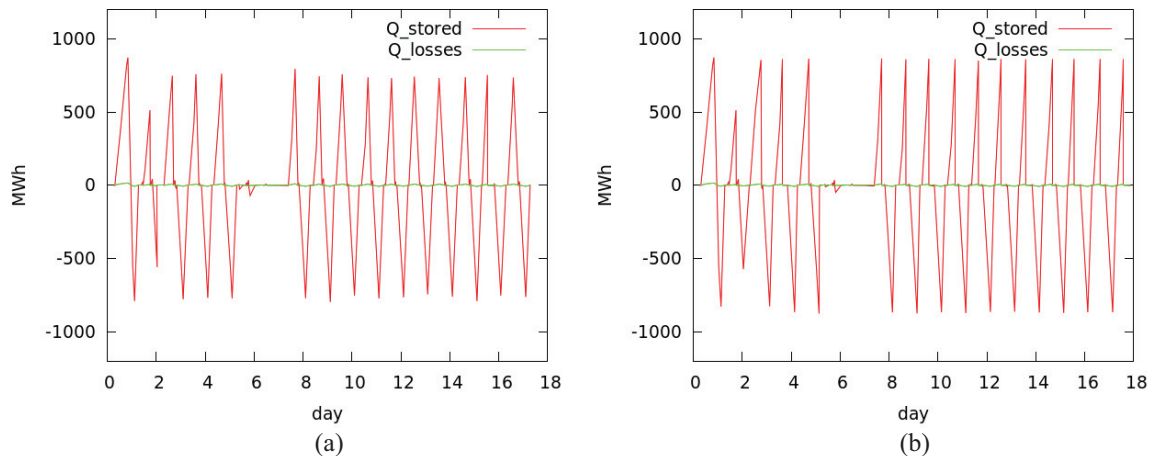

Fig. 3. Energy stored and losses for (a) case A1 and (b) case C1. Values are reset to 0 at the end of each process. Stored energy (red line) has positive values in the charge and negative values in the discharge. Thermal losses (green line) are positive when heat comes out of the packed bed (by conduction through the walls) and negative when it comes in.

In Fig. 3, energy stored and lost in cases A1 and C1 are plotted. It can be seen that in the first day there is a higher amount of stored energy due to the influence of the initial conditions, and how both the stored and delivered energy values are more or less stabilized afterwards. In days 5 and 6, due to the low amount of available irradiation, almost no charging was carried out.

For all cases, the thermal losses are very low (less than 1% of the energy delivered to the PB by the TES), which is an indication of having enough thermal insulation. Due to the transient operation of the tanks, in the discharge processes heat through the tank walls comes into to the packed bed instead of coming out, and therefore, the walls act as additional thermal storage[c].

5. Conclusions

Numerical simulations have been performed in order to assess the thermal performance of some thermocline-like thermal energy storage systems for a CSP plant similar to Andasol 1 in Seville, Spain. A modular object-oriented methodology has been used for coupling the different numerical models for the components of a TES system, such as the tank walls, foundation and the storage media (filler material and HTF).

Ideal molten salt two-tank system has been adopted as the reference design, while different filler material configurations have been tested for the thermocline prototypes (solid, encapsulated PCM and multi-layered solid-PCM). Tests have been performed in a period of 17 days in summer, using weather data from Seville, Spain.

---

[c] This extra thermal capacity is not taken into account in the values of Table 7.

Thermal losses to the ambient are observed to be very low for all the cases (less than 1%).

As in previous works, the MLSPCM shows to be promising as an alternative to the other tested configurations, as well as to the standard two-tank system. Performance analysis indicates that MLSPCM prototype C2 is equivalent to the two-tank molten salt system in terms of energy and exergy delivered. However, the former system consists of a tank only 32% higher than one tank of the latter (which uses two tanks), requiring around 32% less amount of molten salt. A solid-filled thermocline system with the same dimensions (case A2), results in 10% less exergy delivered to the power block.

Acknowledgements

References

[1] P. A. Galione, C. D. Pérez-Segarra, I. Rodríguez, O. Lehmkuhl, J, Rigola. A new thermocline-PCM thermal storage concept for CSP plants. Numerical analysis and perspectives. SolarPaces Concentrating Solar Power and Chemical Energy Systems, (2013) Las Vegas, USA

[2] P. Galione, C.D. Pérez-Segarra, I. Rodríguez, O. Lehmkuhl, J. Rigola, A. Oliva. Numerical modeling and experimental validation of encapsulated PCM Thermal Energy Storage tanks for Concentrated Solar Power Plants. Eurotherm Seminar 99, Advances in Thermal Energy Storage, (2014) Lleida, Spain.

[3] Damle, R., Lehmkuhl, O., Colomer, G., Rodríguez, I. Energy simulation of buildings with a modular object-oriented tool. Proceedings of the ISES World Conference. (2011).

[4] Wakao N, Kaguei S, Funazkri T. Effect of fluid dispersion coefficients on particle-to-fluid heat transfer coefficients in packed beds. Chem. Eng. Sci. 1979; 34: 325-336.

[5] Rodríguez, I., Pérez-Segarra, C.D., Lehmkuhl, O., Oliva, A. Modular object-oriented methodology for the resolution of molten salt storage tanks for CSP plants. Applied Energy, Vol. 109, (2013), pp. 402-414.

[6] S. Torras, C.D. Pérez-Segarra, I. Rodríguez, J. Rigola and A. Oliva. Parametric study of two-tank TES systems for CSP plants. International Conference on Concentrating Solar Power and Chemical Energy Systems, SolarPACES (2014).

[7] METEONORM 4.0, 1999, Meteotest Fabrikstrasse 14, CH-3012 Bern, Switzerland.

[8] Solar Millenium AG. The parabolic trough power plants Andasol 1 to 3. The largest solar power plants in the world –Technology premiere in Europe (2008). www.SolarMillennium.de.